Control of cambium initiation and activity in Arabidopsis by the transcriptional regulator AHL15

Rahimi, A.; Karami, O.; Lestari, A.D.; Werk, T. de; Amakorová, P.; Shi, D.; ... ; Offringa, R.

Article

Current Biology

Control of cambium initiation and activity in *Arabidopsis* by the transcriptional regulator AHL15

Highlights

- AHL15 promotes wood formation (secondary growth) in *Arabidopsis* inflorescence stems
- *AHL15* acts downstream of the floral activators SOC1 and FUL
- AHL15-enhanced cytokinin levels induce secondary growth and branching
- AHL15 operates in parallel to and is dependent on the TDIF-PXY-WOX pathway

Authors

Arezoo Rahimi, Omid Karami, Angga Dwituti Lestari, ..., Ondřej Novák, Thomas Greb, Remko Offringa

Correspondence

o.karami@biology.leidenuniv.nl (O.K.), r.offringa@biology.leidenuniv.nl (R.O.)

In brief

Is there a gene that differentiates between a short-lived herbaceous or a long-lived woody plant? Rahimi et al. show that the *Arabidopsis* longevity-enhancing AHL15 protein also promotes wood formation in stems. Elevated *AHL15* expression turns the short-lived herbaceous *Arabidopsis* into a long-lived woody plant by promoting cytokinin biosynthesis.

Rahimi et al., 2022, Current Biology *32*, 1764–1775
April 25, 2022
https://doi.org/10.1016/j.cub.2022.02.060

CellPress

CellPress

Current Biology

Article

Control of cambium initiation and activity in *Arabidopsis* by the transcriptional regulator AHL15

Arezoo Rahimi,[1] Omid Karami,[1,*] Angga Dwituti Lestari,[1] Tobias de Werk,[1,2] Petra Amakorová,[3] Dongbo Shi,[4] Ondřej Novák,[3] Thomas Greb,[4] and Remko Offringa[1,5,6,*]

[1]Plant Developmental Genetics, Institute of Biology Leiden, Leiden University, Sylviusweg 72, 2333 BE Leiden, the Netherlands
[2]Max Planck Institute of Molecular Plant Physiology, Am Mühlenberg 1, 14476 Potsdam, Germany
[3]Laboratory of Growth Regulators, Faculty of Science, Palacký University and Institute of Experimental Botany, The Czech Academy of Sciences, 78371 Olomouc, Czech Republic
[4]Department of Developmental Physiology, Centre for Organismal Studies (COS), Heidelberg University, 69120 Heidelberg, Germany
[5]Twitter: @OffringaRemko
[6]Lead contact
*Correspondence: o.karami@biology.leidenuniv.nl (O.K.), r.offringa@biology.leidenuniv.nl (R.O.)
https://doi.org/10.1016/j.cub.2022.02.060

SUMMARY

Plant secondary growth, which is the basis of wood formation, includes the production of secondary xylem, which is derived from meristematic cambium cells embedded in vascular tissue. Here, we identified an important role for the *Arabidopsis thaliana* (Arabidopsis) AT-HOOK MOTIF CONTAINING NUCLEAR LOCALIZED 15 (AHL15) transcriptional regulator in controlling vascular cambium activity. The limited secondary xylem development in inflorescence stems of herbaceous Arabidopsis plants was significantly reduced in *ahl15* loss-of-function mutants, whereas constitutive or vascular meristem-specific *AHL15* overexpression produced woody inflorescence stems. *AHL15* was required for enhanced secondary xylem formation in the woody *suppressor of overexpression of constans 1* (*soc1*) *fruitfull* (*ful*) double loss-of-function mutant. Moreover, we found that AHL15 induces vascular cambium activity downstream of the repressing SOC1 and FUL transcription factors, most likely similar to how it enhances lateral branching by promoting biosynthesis of the hormone cytokinin. Our results uncover a novel pathway driving cambium development, in which *AHL15* expression levels act in parallel to and are dependent on the well-established TDIF-PXY-WOX pathway to differentiate between herbaceous and woody stem growth.

INTRODUCTION

Throughout their lifespan, plants can dynamically change their growth and development in response to environmental signals, and this allows them to adapt and survive adverse conditions. In many flowering plants, but especially in woody plant species, stems show two distinct developmental growth processes. The increase in stem length and the establishment of the primary vascular meristem that is arranged into vascular bundles in young stems are known as primary growth. Each bundle contains a primary vascular meristem, or procambium, that generates primary xylem toward the center and primary phloem toward the periphery of the stem.[1] Later in development, when primary stem growth is completed, the procambium and its neighboring interfascicular parenchyma cells (between the vascular bundles) differentiate into the cambial meristem, eventually forming a continuous cylinder of stem cells in the primary plant stem. This then initiates the process of secondary growth, during which the cambial meristem continuously generates secondary xylem toward the inside of the stem and secondary phloem toward the outside of the stem, resulting in radial stem expansion.[2] Secondary growth induced woodiness not only provides sturdiness to stems, allowing plants to grow taller[1] but has also been linked to more harsh growth conditions requiring drought tolerance.[3,4]

Secondary vasculature production is performed by cambial initials located at the center of the cambial zone that undergo two types of cell division: (1) periclinal cell division giving rise to proliferating derivatives called phloem and xylem mother cells, and (2) anticlinal cell division supporting the increase in circumference of the cambial zone.[5] The vascular cambium is an important meristem. On the one hand, it produces vascular tissues that transport water and nutrients throughout the plant body. In contrast, through secondary growth, it provides mechanical support for the plant body by generating lignified wood cells. The rate of cell division of the cambial stem cells determines the amount of secondary growth and, thus, whether and how much wood is formed. In view of the use of wood as a building material and renewable energy source, there is an obvious demand for an understanding of the genetic mechanisms that control the cambium activity.[5]

The model plant *Arabidopsis thaliana* (Arabidopsis) is herbaceous, but it undergoes secondary growth in the hypocotyl, root, or stem.[1,6] In contrast to woody plants that already produce

a ring of xylem in young stems, Arabidopsis plants produce only a limited amount of xylem without forming a xylem ring in young stems. Secondary growth does occur in older Arabidopsis inflorescence stems and is generally quantified by the number of secondary xylem cell files produced by cambial cell divisions in the interfascicular part of the stem (the area between two bundles).[1,7]

Most of our current understanding of secondary growth comes from studies in Arabidopsis and in model trees, such as poplar (*Populus* ssp). These studies have revealed a number of molecular factors and genetic components that are involved in the establishment and proliferation of cambium cells.[1,8] The TDIF-PXY-WOX pathway is the best-studied signaling pathway that controls cambium activity. The peptide ligand CLE41/44/TRACHEARY ELEMENT DIFFERENTIATION INHIBITORY FACTOR (TDIF) is synthesized in the phloem and diffuses through the apoplastic space to cambium cells, where it binds to its cognate receptor PHLOEM INTERCALATED WITH XYLEM (PXY). PXY subsequently promotes the proliferation of cambium cells by activating the expression of the cambium-specific *WUSCHEL-RELATED HOMEOBOX* genes *WOX4* and *WOX14*.[9–11] The *WOX4* transcription factor promotes stem cell proliferation by interacting with the GRAS domain transcription factor HAIRY MERISTEM 4 (HAM4).[12]

Cambium activity is also known to be regulated by a hormonal signaling network involving the plant hormones auxin and cytokinin as major positive regulators of cambial cell proliferation. Detailed hormone measurements across the cambial zone, first in pine and later in poplar, have shown that auxin levels peak in the cambium with a decreasing gradient toward the phloem and xylem, and that cytokinin levels are high in cambial cells as well with a peak in the developing phloem.[13,14] Auxin and cytokinin interact in several feedback loops, with e.g., cytokinin promoting PIN-mediated auxin efflux from the cambium to the developing xylem, where auxin through MONOPTEROS/AUXIN RESPONSE FACTOR 5 (MP/ARF5) and the downstream TARGET OF MONOPTEROS 5 (TMO5) induces cytokinin biosynthesis by LONELY GUY 3 (LOG3) and LOG4, which subsequently diffuses to the cambium to promote periclinal cell divisions. At the same time, MP/ARF5 also inhibits cytokinin signaling in the xylem, whereas it restricts cambial cell divisions by directly dampening the expression of *WOX4*.[15] The Arabidopsis *ipt1,3,5,7* quadruple mutant, in which four of the genes encoding the key enzyme ISOPENTENYL TRANSFERASE (IPT) involved in cytokinin biosynthesis have been knocked out, completely lacks cambial activity both in the shoot and root, but this can be rescued by treatment with exogenous cytokinin.[16] Moreover, the expression of a cytokinin catabolic gene in poplar led to a remarkable decrease in cambial cell divisions and thinner trunks.[14] By contrast, increasing cytokinin levels in poplar stems by overexpressing *IPT7* under the wood-specific *LMX5* promoter strongly stimulated cambial cell divisions and biomass production.[14] In addition, it was shown that secondary growth in Arabidopsis roots is dependent on the cytokinin-responsive transcription factor AINTEGUMENTA (ANT) and the D-type cyclin CYCD3;1, which are both expressed in the vascular cambium.[17,18] Moreover, in the Arabidopsis *soc1 ful* double loss-of-function mutant, xylem formation is significantly enhanced, resulting in the formation of a xylem ring even in young inflorescence stems.[19] This suggests that SOC1 and FUL repress cambium ring formation and secondary growth; however, what is downstream of these transcription factors is still unknown. Despite this increasing knowledge, the connection between the different players and the exact signals that initiate the formation of the cambium ring and regulate the amount of secondary growth, and thus differentiate between woody and non-woody species, remains unclear.

Here, we identified a new role for the Arabidopsis *AT-HOOK MOTIF CONTAINING NUCLEAR LOCALIZED 15* (*AHL15*) gene as an important regulator of cambial activity and secondary xylem formation. AHL15 is part of a plant-specific protein family, containing a single AT-hook DNA binding motif and a plant and prokaryote conserved (PPC) domain.[20,21] *AHL15* homologs have been implicated in several aspects of plant growth and development in Arabidopsis, including flowering time and hypocotyl growth,[22,23] flower development,[24] vascular tissue differentiation,[25] and gibberellin biosynthesis.[26] In addition, we have recently shown that *AHL15* and its family members play key roles in plant embryogenesis[27] and longevity.[28] Apart from promoting plant longevity, we also discovered that *AHL15* enhances secondary growth. A more detailed analysis indicated that *AHL15* regulates vascular cambium initiation and activity in Arabidopsis, most likely by linking the action of the upstream flowering genes *SOC1* and *FUL* to the downstream cytokinin biosynthesis genes *IPT3*, *IPT7*, and *LOG4*.

RESULTS

AHL15 promotes secondary growth in Arabidopsis inflorescence stems

Wild-type Arabidopsis axillary meristems (AMs) undergo maturation similar to shoot apical meristems (SAMs). Young immature AMs are vegetative and produce leaves, whereas upon flowering all AMs mature into reproductive inflorescence meristems. In contrast, Arabidopsis *soc1 ful* double mutant plants show extended longevity by the maintenance of vegetative growth from some of these AMs.[19] Recently, we have shown that overexpression of the Arabidopsis *AHL15* gene (e.g., $35S_{pro}$*:AHL15*) also increases plant longevity (Figure 1A), similar to *soc1 ful* plants, and that *AHL15* acts downstream of the SOC1 and FUL transcription factors in maintaining AMs in the vegetative phase.[28] The *soc1 ful* plants also develop woody inflorescence stems, and in view of our recent findings, we analyzed whether secondary growth and xylem formation were also enhanced in $35S_{pro}$*:AHL15* inflorescence stems. One month after bolting, $35S_{pro}$*:AHL15* stems displayed a significant increase in xylem formation compared with wild-type stems (Figure 1B). Secondary xylem formation continued in $35S_{pro}$*:AHL15* stems 2 and 3 months after bolting, whereas it stopped in wild-type stems 2 months after bolting (Figures 1B and 1C). These results suggest that AHL15 maintains cambium activity and thereby enhances secondary growth in Arabidopsis inflorescence stems.

Arabidopsis inflorescence stems normally produce more secondary xylem than secondary phloem,[29] and we used the width of the secondary xylem produced as a measure for secondary growth. Lignin staining showed that 1 month after bolting, inflorescence stems of $35S_{pro}$*:AHL15* plants produced more lignified xylem cells in the interfascicular region than those of wild-type plants (Figures 1E and 1F). In contrast, *ahl15* loss-of-function

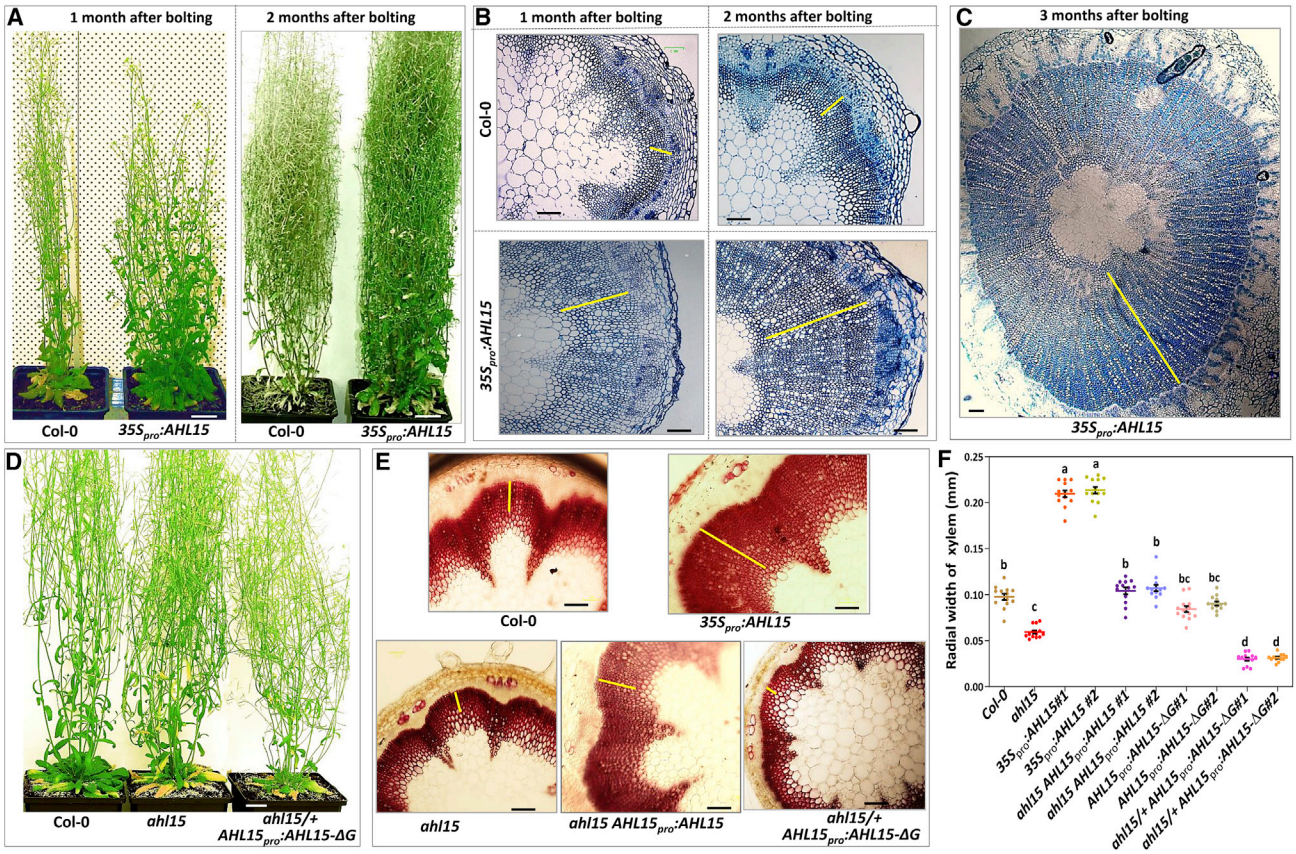

Figure 1. *AHL15* promotes secondary growth in Arabidopsis inflorescence stems

(A) Plant shoot phenotype of a 2-month-old wild-type and a 3-month-old *35S$_{pro}$:AHL15* plant (left panel), and a 3-month-old wild-type and a 4-month-old *35S$_{pro}$:AHL15* plant (right panel).

(B) Toluidine blue-stained cross-sections of the bottom-most internode of an inflorescence stem of a 2-month-old wild-type and a 3-month-old *35S$_{pro}$:AHL15* plant (1 month after bolting, left panel), and of a 3-month-old wild-type and a 4-month-old *35S$_{pro}$:AHL15* plant (2 months after bolting, right panel).

(C) Toluidine blue-stained cross-section of the bottom-most internode of an inflorescence stem of a 5-month-old *35S$_{pro}$:AHL15* plant (3 months after bolting).

(D) Shoot phenotype of a 2-month-old wild-type (left), *ahl15* mutant (middle), and *ahl15*/+ *AHL15$_{pro}$:AHL15-ΔG* mutant (right) plant.

(E) Phloroglucinol-stained fresh cross-sections of the bottom-most internode of an inflorescence stem of a 61-day-old wild-type (upper panel left), a 85-day-old *35S$_{pro}$:AHL15* (upper panel right), a 61-day-old *ahl15* (lower panel left), a 61-month-old *AHL15$_{pro}$:AHL15 ahl15* (lower panel middle), and a 56-day-old *ahl15*/+ *AHL15$_{pro}$:AHL15-ΔG* (lower panel right) plant (1 month after bolting).

(F) Quantification of the radial width of the interfascicular xylem (IX) of the bottom-most internode of the main inflorescence stems based on sections as shown in (E). Colored dots indicate the average radial IX width of three random interfascicular regions measured in a single cross-section. Cross-sections of 12 independent plants were measured. Horizontal lines indicate the mean and error bars indicate the SEM. Different letters indicate statistically significant differences ($p < 0.01$) as determined by a one-way ANOVA with Tukey's honest significant difference post hoc test.

The yellow bars in (B), (C), and (E) mark the xylem width in the interfascicular cell domain. Scale bars, 2 cm (A and D) and 0.06 mm (B, C, and E). For (A)–(E), similar results were obtained from two independent experiments.

See also Figures S1 and S2.

mutant stems contained significantly less lignified xylem cells in the interfascicular region than wild-type stems (Figures 1D–1F). These *ahl15* plants flowered at the same time and showed a mildly enhanced AM maturation compared with wild-type plants.[28] Introduction of the *AHL15$_{pro}$:AHL15* genomic clone into the *ahl15* mutant background completely restored the secondary xylem growth to wild-type levels (Figures 1D–1F), indicating that the reduction in xylem cell numbers was caused by *ahl15* loss of function.

Previous studies have shown that expression of a mutant AHL protein (AHL15-ΔG), from which the conserved six-amino-acid sequence (GRFEIL) in the PPC domain was deleted, leads to a dominant-negative effect in the heterozygous ahl15/+ mutant background that overcomes the functional redundancy between the different *AHL* family members.[21,28] Whereas *AHL15$_{pro}$:AHL15-ΔG* plants showed wild-type development as previously reported,[28] *ahl15*/+ *AHL15$_{pro}$:AHL15-ΔG* plants flowered earlier and showed a strong enhancement in AM maturation compared with wild-type plants[28] and developed even less secondary xylem compared with *ahl15* plants (Figures 1E and 1F). The diameter of *ahl15* stems was already smaller than wild-type stems, but *ahl15*/+ *AHL15$_{pro}$:AHL15-ΔG* stems remained even smaller in size (Figure S1). Except for the difference in cambium activity, mutant stems showed the same structure and tissue organization as wild-type stems (Figure S2). These results show that

AHL15 plays an important role in maintaining cambium activity and secondary growth in Arabidopsis inflorescence stems, and that as in developmental processes, such as embryogenesis and AM maturation,[27,28] it acts partially redundant with other *AHL* genes.

SOC1/FUL-repressed cambium-specific *AHL15* expression regulates secondary growth

The above results suggest that *AHL15* is expressed in the vascular cambium area, where it regulates cambial cell division activity. Histochemical staining of plants carrying the *AHL15* promoter β-glucuronidase (GUS) reporter (*AHL15$_{pro}$:GUS*) indicated that 1 week after bolting, *AHL15* is expressed in almost all tissues in inflorescence stems (Figure 2A) and that the expression remains relatively stable in the interfascicular cambium zone during stem maturation compared with the newly formed xylem precursor or phloem cells (Figure 2A). Interestingly, *AHL15* expression is completely absent from the secondary xylem, whereas it remains expressed in the phloem and the primary xylem and xylem fibers of the inflorescence stem (Figure 2A).

In order to confirm that *AHL15* is expressed in the vascular cambium, we used the tissue-specific gene expression atlas generated from different tissues in the second bottom-most internode of Arabidopsis inflorescence stems 3 weeks after bolting (Figure 2B) by combining fluorescence-activated nucleus sorting (FANS) and laser-capture microdissection with next generation RNA sequencing.[30] Based on this gene expression atlas, *AHL15* expression showed a pattern similar to that observed in the *AHL15$_{pro}$:GUS* reporter in inflorescence stems at 2–4 weeks after bolting (Figures 2A and 2B). The expression of *AHL15* in the *PXY* and *SUPPRESSOR OF MAX2 1-LIKE 5* (*SMXL5*) cambium sub-domains, the areas where cell division is taking place,[31] further supports the role of *AHL15* in promoting vascular cambium activity.

Altogether, the seeming expression of *AHL* genes in the stem cambium zone supports their role in the regulation of cambium activity. To establish whether *AHL* expression in the Arabidopsis vascular cambium is rate-limiting for secondary growth, we expressed *AHL15* under control of the cambium-specific *PXY* promoter (*PXY$_{pro}$:AHL15*).[32] Lignin-stained 1-month-old *PXY$_{pro}$:AHL15* stems showed a significant increase in secondary xylem development compared with wild-type stems (Figures 2C and 2D). These results indicate that in wild-type Arabidopsis, secondary growth and xylem development are limited by *AHL* expression, and that cambium-specific enhancement of *AHL15* expression is sufficient to promote cambium activity. Apart from the enhanced cambium activity, *PXY$_{pro}$:AHL15* plants developed and flowered like wild-type plants (Figure S3), indicating that the effect of locally enhanced *AHL15* expression on cambium activity is direct, and not caused by changes in developmental timing.

When *35S$_{pro}$:AHL15-GR* Arabidopsis plants[28] were DEX treated 2 weeks after bolting, inflorescence stems showed a significant increase in secondary xylem development 1 week after treatment compared with those of the mock treated plants (Figures 2E and 2F), confirming the direct effect of AHL15 on cambium activity.

Previously, we have shown that *AHL15* expression is repressed by binding of the SOC1 and FUL MADS box transcription factors to its up- and downstream genomic regions, and that alleviation of this repression in the *soc1 ful* double mutant leads to delayed maturation of AMs, resulting in the mutant aerial rosette phenotype.[28] Comparison of *soc1 ful* double mutant with *soc1 ful ahl15* triple mutant stems showed that the high secondary xylem production in *soc1 ful* stems is dependent on the presence of a functional *AHL15* gene. The interfascicular secondary xylem formation was reduced to wild-type levels in the *soc1 ful ahl15* triple mutant (Figures 3A and 3B). This is in line with the previously observed enhanced expression of *AHL15* in *soc1 ful* mutant AMs.[28] The similar expression pattern of *AHL15* with *SOC1* and *FUL* in the *PXY* and *SMXL5* cambium sub-domains (Figure 3C) further supports the negative regulation of *AHL15* by the SOC1 and FUL transcription factors in cambium-related domains, which limits secondary growth in the herbaceous wild-type Arabidopsis.

AHL15 probably acts upstream of cytokinin biosynthesis in promoting the formation and activity of the cambium ring

In Arabidopsis inflorescence stems, secondary growth is initiated by the occurrence of interfascicular cambium, leading to the formation of a cambium ring. The initial cell division marking the starting point of interfascicular cambium formation can be readily observed in 1-week-old wild-type stems, but these are absent in 1-week-old *ahl15* loss-of-function stems (a noticeable feature of this mutant), despite a normal organization of the mutant stem tissue (Figure 4A). In contrast, 1-week-old *35S$_{pro}$:AHL15* inflorescence stems already showed a cambium ring consisting of several layers of cells in the interfascicular region (Figure 4A). These results indicate an important role for *AHL15* in cambium initiation and the promotion of cambial cell divisions.

The plant hormones auxin and cytokinin have been shown to be involved in promoting cell divisions in the vascular cambium.[1,14–16] However, the expression of the *DR5$_{pro}$:GFP* auxin response reporter[33] did not show a clear difference in 4- and 8-day-old inflorescence stems of wild-type or *35S$_{pro}$:AHL15* plants (Figure S4), indicating that the enhanced secondary growth by *AHL15* overexpression cannot be explained by an obvious change in auxin response dynamics. We therefore compared the expression of the cytokinin response reporter *TCS$_{pro}$:GFP*[34] in wild-type, *ahl15*, or *35S$_{pro}$:AHL15* inflorescence stems during cambium development. Two days after bolting, only weak *TCS$_{pro}$:GFP* expression could be detected in the procambium zone of inflorescence stems of all three genetic backgrounds, indicating that *AHL15* does not modulate the cytokinin response in these very young stems (Figure 4B, left images). However, 3 days later, when *TCS$_{pro}$:GFP* signals started to appear in the interfascicular regions of wild-type stems, *TCS$_{pro}$:GFP* expression was still limited to the procambium in *ahl15* stems, whereas *35S$_{pro}$:AHL15* stems displayed a ring of *TCS$_{pro}$:GFP* signal colocalizing with the cambium ring already present in these stems (Figure 4B, middle images). Ten days after bolting, these overlapping rings of cambium and *TCS$_{pro}$:GFP* expression also became visible in wild-type stems and were even stronger in *35S$_{pro}$:AHL15* stems (Figure 4B, right images), but remained restricted to the cambium in the vascular bundles of *ahl15* stems (Figure 4B, right images). These results suggest

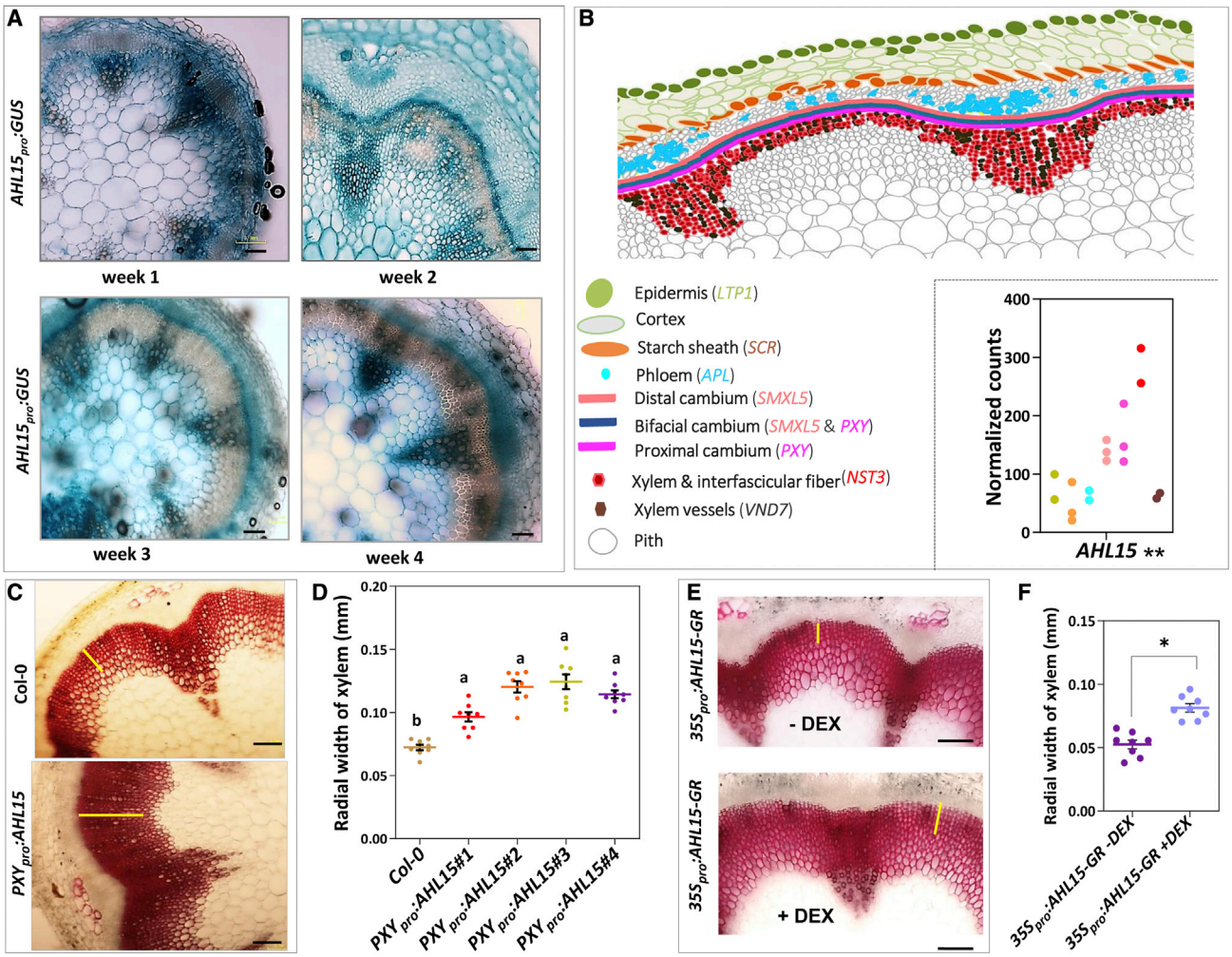

Figure 2. Cambium-specific *AHL15* expression promotes secondary xylem formation

(A) Cross-sections of GUS-stained bottom-most internodes of inflorescence stems 1, 2, 3, and 4 weeks after bolting, showing the expression pattern of the $AHL15_{pro}$:*GUS* reporter.

(B) Upper panel: schematic representation of part of a cross-section of an inflorescence stem, including the vascular bundle and the interfascicular regions in which different stem tissues and the tissue-specific expression domains of marker genes used for stem transcriptome profiling are indicated, as described in the legend below: *NST3* (fibers), *VND7* (xylem vessels), *PXY* (proximal and bifacial cambium), *SMXL5* (bifacial and distal cambium), *APL* (phloem), *SCR* (starch sheath), and *LTP*1 (epidermal cells). The gene expression atlas was generated from the second internode of the primary inflorescence 3 weeks after bolting by combining laser-capture microdissection with fluorescence-activated nucleus sorting (FANS), using the promoter-H4-GFP fusions of the indicated marker genes and next generation RNA sequencing.[30] Lower panel: normalized read counts of the *AHL15* gene in the tissue domains defined in the upper panel. Colored dots indicate the values of two or three biological replicates of RNA isolation. Asterisks indicate that the *AHL15* gene is significantly differentially expressed among the seven tissue domains ($p < 0.01$), as determined by the likelihood ratio test.[30]

(C) Phloroglucinol-stained fresh cross-sections of the bottom-most internode of the main inflorescence of a 2-month-old wild-type (upper panel) and PXY_{pro}:*AHL15* (lower panel) plant (1 month after bolting). The yellow bars mark the radial width of the IX.

(D) Quantification of the radial IX width in the bottom-most internode of the main inflorescence of 2-month-old wild-type and PXY_{pro}:*AHL15* (four individual lines) plants (1 month after bolting). Different letters indicate statistically significant differences ($p < 0.01$) as determined by a one-way ANOVA with Tukey's honest significant difference post hoc test.

(E) Phloroglucinol-stained fresh cross-sections of the bottom-most internode of the main inflorescence of 2-month-old $35S_{pro}$:*AHL15-GR* plants 1 week after spraying with water (mock, upper panel) or 20 μM DEX (lower panel) at 2 weeks after bolting. The yellow bars mark the radial width of the IX.

(F) Quantification of the radial width of the IX in the bottom-most internode of the main inflorescence of 2-month-old $35S_{pro}$:*AHL15-GR* plants using cross-sections as shown in (E).

The asterisk indicates the significant difference between mock- and DEX-treated plants (Student's t test, $*p < 0.01$). In (D) and (F), colored dots indicate the average radial IX width of three random interfascicular regions measured in a single cross-section. Cross-sections of six to eight independent plants were measured. Horizontal lines indicate the mean and error bars indicate the SEM. Scale bars in (A), (C), and (E) indicate 0.06 mm. For (A) and (C), similar results were obtained from three independent experiments.

See also Figure S3.

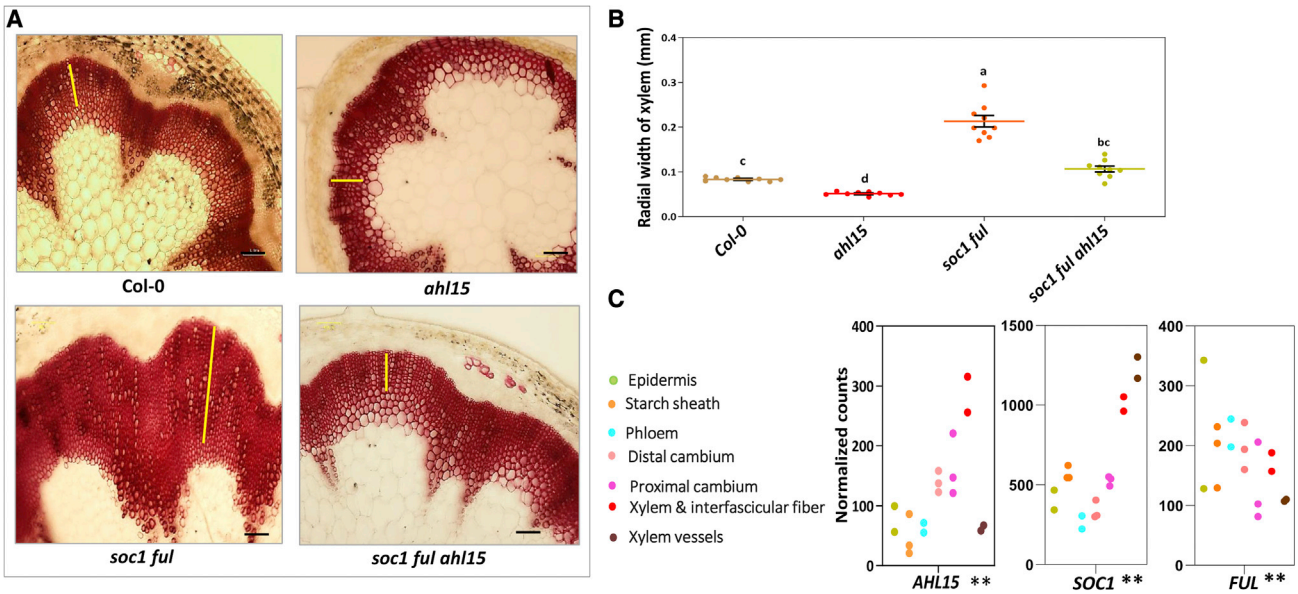

Figure 3. *AHL15* is required for enhanced secondary xylem formation in the *soc1 ful* double mutant

(A) Phloroglucinol-stained fresh cross-sections of the bottom-most internode of the main inflorescence of a 2-month-old wild-type (upper panel, left) and *ahl15* (upper panel, right) plant, and a 3-month-old *soc1 ful* (lower panel, left) and *soc1 ful ahl15* (lower panel, right) plant (1 month after bolting). The yellow bars mark the xylem width in the interfascicular cell domain. Scale bars, 0.06 mm. Similar results were obtained from two independent experiments.

(B) Quantification of the IX width in the bottom-most internode of the main inflorescence of wild-type, *ahl15*, *soc1 ful*, and *soc1 ful ahl15* plants using sections as shown in (A). Colored dots indicate the average radial IX width of three random interfascicular regions measured in a single cross-section. Cross-sections of nine independent plants were measured. Horizontal lines indicate the mean and error bars indicate the SEM. Different letters indicate statistically significant differences ($p < 0.01$) as determined by a one-way ANOVA with Tukey's honest significant difference post hoc test.

(C) Co-expression of *AHL15*, *SOC1*, and *FUL* in cambium and vascular bundle domains. Colored dots indicate normalized gene read counts of the indicated genes among seven different tissues for two or three replicated RNA isolations. Asterisks indicate that genes are significantly differentially expressed among the seven tissue domains ($p < 0.01$), as determined by the likelihood ratio test.[30]

that AHL15 might regulate cambium initiation and promote the cambial cell division rate in Arabidopsis stems by altering cytokinin biosynthesis or response.

Analysis of the effect of *AHL15* on cytokinin biosynthesis[35,36] by qPCR experiments showed that the expression of *IPT3*, *IPT7*, and *LOG4* was significantly reduced in *ahl15* stems (Figure 4C), suggesting that *AHL15* may act by activating these cytokinin biosynthesis genes in the cambium area. This was further substantiated by the co-expression of *AHL15*, *IPT3*, *IPT7*, *LOG4*, and *LOG5* in the *PXY* and/or *SMXL5* cambium sub-domains (Figure S5).

Next we compared the concentrations of the two major active forms of cytokinins in Arabidopsis, N^6-(Δ^2-isopentenyl) adenine (iP) and trans-zeatin (tZ),[37] of which the inactive riboside forms are generated by the IPT enzymes and formation of the free active forms is catalyzed the LOG enzymes,[37] in wild-type, *ahl15*, and $35S_{pro}$*:AHL15* inflorescence stems. Both the iP and tZ levels were significantly lower in the *ahl15* mutant compared with wild-type stems, whereas the iP levels were significantly increased in $35S_{pro}$*:AHL15* stems (Figure 4D), in line with a role for AHL15 in stimulating cytokinin biosynthesis.

To verify that the reduced secondary xylem formation in *ahl15* mutant stems was caused by a reduced cytokinin biosynthesis, we introduced the *Agrobacterium tumefaciens IPT* gene under the control of the cambium-specific *PXY* promoter (PXY_{pro}*:IPT*) in the *ahl15* mutant background. The presence of the PXY_{pro}*:IPT* construct significantly increased the width of interfascicular lignified xylem in *ahl15* stems, bringing it back to wild-type or even higher levels (Figures 4E and 4F). These data lead us to propose a model in which local expression of *AHL15* determines the initiation and activity of interfascicular cambium and thereby the secondary growth of Arabidopsis inflorescence stems by promoting cytokinin biosynthesis.

AHL15 promotes lateral branching, probably also by increasing cytokinin biosynthesis

In our previous study we have shown that AM maturation from the vegetative to the reproductive phase is regulated by the level of *AHL15* expression.[28] We also noticed that plants with enhanced *AHL15* expression, apart from the delay in AM maturation, also showed more branching.[28] Moreover, the *ahl15* loss-of-function mutant showed a significant reduction in the number of AMs in the axils of cauline leaves growing out into lateral buds, resulting in a significant decrease in the total number of lateral branches (Figures S6A and S6B). The outgrowth of AMs into axillary buds and lateral branches depends on their activation from dormancy,[38] which is known to be inhibited by the plant hormones auxin and strigolactones and to be promoted by cytokinin.[38,39] The Arabidopsis *MYB DOMAIN PROTEIN 2* (*AtMYB2*) gene was shown to inhibit the outgrowth of axillary buds at later stages of development by reducing the endogenous cytokinin levels.[40] Interestingly, when we expressed *AHL15* under control of the *AtMYB2* promoter, transgenic plants produced significantly more lateral branches compared with wild-type plants (Figures S6C and S6D). In view of our model where

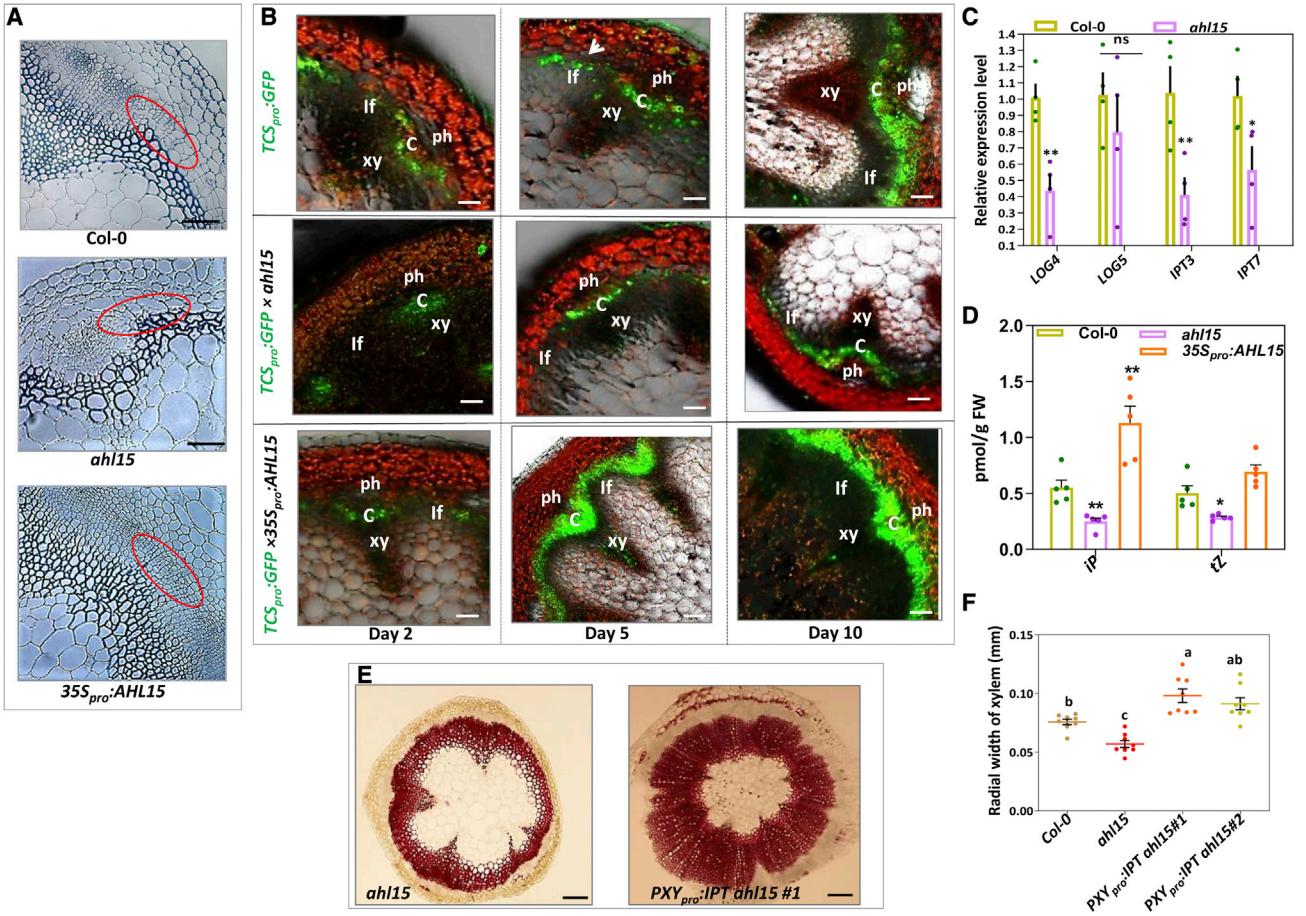

Figure 4. Cytokinin likely acts downstream of *AHL15* to promote cambium activity

(A) Toluidine blue-stained cross-sections of the bottom-most internode of the main inflorescence of a 38-day-old wild-type (upper panel), a 38-day-old *ahl15* (middle panel), and a 62-day-old *35S$_{pro}$:AHL15* (lower panel) plant 1 week after bolting. The red circle marks the cambium cell division area in the interfascicular region, which is absent in the *ahl15* mutant.

(B) Confocal images showing the expression of the *TCS$_{pro}$:GFP* cytokinin response reporter in cross-sections of the bottom-most internode of the main inflorescence 2, 5, and 10 days after bolting in wild-type (upper panel), *ahl15* (middle panel), and *35S$_{pro}$:AHL15* (lower panel) plants. White arrowhead indicates the start point of cambium cell division in wild-type. xy, xylem; ph, phloem; c, cambium; if, intravascular fiber. Images represent an overlay of the green (GFP) and red (chlorophyll) fluorescence and the transmitted light channels.

(C) Relative expression of the cytokinin biosynthesis genes *LOG4*, *LOG5*, *IPT3*, and *IPT7* by qPCR analysis in the bottom-most internode of the main inflorescence of wild-type and *ahl15* plants 10 days after bolting. Dots indicate the values of three to four biological replicates per plant line, bars indicate the mean, and error bars indicate the SEM. Asterisks indicate significant differences between wild-type and *ahl15* plants (*$p < 0.05$, **$p < 0.01$; ns, not significant), as determined by a two-sided Student's t test.

(D) The level of iP and *t*Z cytokinins in the bottom-most internode of the main inflorescence of wild-type, *ahl15*, and *35S$_{pro}$:AHL15* plants 10 days after bolting. Dots indicate the values of five biological replicates per plant line, bars indicate the mean, and error bars indicate the SEM. Asterisks indicate significant differences between wild-type and *ahl15* or *35S$_{pro}$:AHL15* plants (*$p < 0.01$, **$p < 0.001$), as determined by a two-sided Student's t test.

(E) Phloroglucinol-stained fresh cross-sections of the bottom-most internode of the main inflorescence of a 2-month-old *ahl15* (left panel) and *ahl15 PXY$_{pro}$:IPT* (right panel) plant 1 month after bolting.

(F) Quantification of radial width of the IX in the bottom-most internode of the main inflorescence using cross-sections as shown in (E) of wild-type, *ahl15*, and *ahl15 PXY$_{pro}$:IPT* (two independent lines) plants. Colored dots indicate the average radial IX width of three random interfascicular regions measured in a single cross-section. Cross-sections of eight independent plants were measured. Horizontal lines indicate the mean and error bars indicate the SEM. Different letters indicate statistically significant differences ($p < 0.01$), as determined by a one-way ANOVA with Tukey's honest significant difference post hoc test.

Scale bars, 0.05 mm (A), 0.015 mm (B), and 0.15 mm (D). For (A), (B), and (D) similar results were obtained from two independent experiments.

See also Figures S4–S6.

cytokinin biosynthesis is positioned downstream of AHL15 in promoting wood formation, we investigated whether this hormone also acts downstream of *AHL15* in lateral branching. Expression analysis by qPCR showed that the cytokinin biosynthesis genes *IPT3*, *IPT7*, and *LOG5* were significantly upregulated in the rosette base of 6-week-old *MYB2$_{pro}$:AHL15* plants compared with wild-type plants (Figure S6E). These results suggest that *AHL15* promotes lateral branching similar to how it enhances secondary growth by increasing cytokinin biosynthesis.

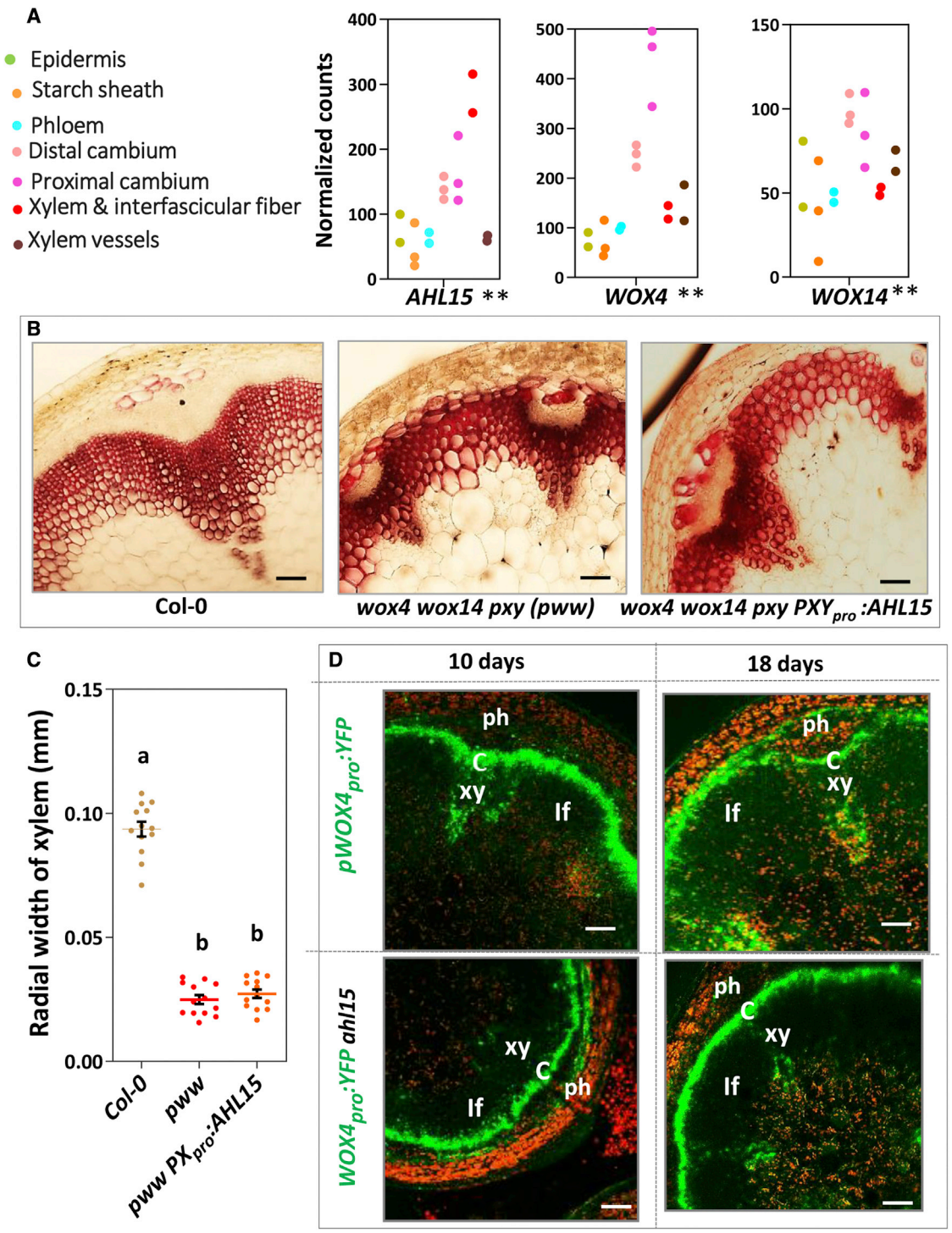

Figure 5. *AHL15*-cytokinin and *PXY-WOX4/14* represent two parallel pathways regulating cambium activity

(A) Co-expression of *AHL15*, *WOX4*, and *WOX14* in cambium and vascular bundle domains. Colored dots indicate normalized gene read counts of the indicated genes among seven different tissues for two or three replicated RNA isolations. Asterisks indicate that genes are significantly differentially expressed among the seven tissue domains ($p < 0.01$), as determined by the likelihood ratio test.[30]

(B) Phloroglucinol-stained fresh cross-sections of the bottom-most internode of the main inflorescence of 2-month-old wild-type (left panel), *pxy wox4 wox14* (pww, middle panel), and *pww PXY$_{pro}$:AHL15* (right panel) plants 1 month after bolting.

(C) Quantification of radial width of the IX in the bottom-most internode of the main inflorescence of wild-type (Col-0), *pww*, and *pww PXY$_{pro}$:AHL15* plants using cross-sections as shown in (B).

(legend continued on next page)

AHL15 acts in parallel to and is depending on the PXY-WOX pathway for promoting secondary growth

In Arabidopsis inflorescence stems, the *WUSCHEL HOMEOBOX RELATED 4* (*WOX4*) and *WOX14* genes have been shown to promote the rate of cell division in the vascular cambium.[9–11] Inflorescence stems from the *wox4 wox14* double mutant develop significantly less secondary xylem in the interfascicular regions.[41] In view of the co-expression of *WOX4*, *WOX14*, and *AHL15* in the *PXY* and *SMXL5* cambium sub-domains (Figure 5A) and the fact that loss-of-function mutant inflorescence stems show similar defects in cambium development, we investigated the genetic interaction between *AHL15* and *WOX4/WOX14* in controlling secondary xylem growth. Introduction of PXY_{pro}*:AHL15*#3 by crossing into the *wox4 wox14 pxy* mutant background did not lead to enhanced secondary growth (Figure 5B). This result indicated that *AHL15* is not responsible for promoting cell division downstream of *WOX4* and *WOX14* and at the same time that AHL15 requires a functional PXY-WOX pathway to enhance cambial development. In turn, the $WOX4_{pro}$*:GFP* reporter, which labels the vascular bundles and the cambium cells in wild-type stems,[42] did not show a clear difference in *ahl15* mutant inflorescence stems, indicating that the *WOX* genes are not downstream of AHL15 (Figure 5C). Based on these experiments, we conclude that PXY-WOX and SOC1/FUL-AHL15 are parallel pathways that are mutually required to promote cell division in the interfascicular cambium of Arabidopsis inflorescence stems.

DISCUSSION

Understanding the molecular mechanisms that regulate the activity and functioning of vascular cambium is important from both a fundamental and an applied perspective. On the one hand, the bidirectional cambium meristem is unique from a developmental point of view. Knowing the pathways that regulate the activity of its stem cells should identify the genetic drivers that differentiate between herbaceous and woody species during plant evolution. In contrast, directing the cell division rate of the stem cells of the vascular cambium will provide quantitative and qualitative control over the production of wood as biomaterial, and may also be used to enhance drought resistance in crops.[1,2,4–6] Although previous studies have provided important insights into the molecular mechanisms regulating cambial activity, the current models are far from complete.[1,2,5,6] For example, the flowering time genes *SOC1* and *FUL* that have been identified as clear repressors of cambial activity[19] are often not included.

In this study, we present the role of *AHL15* as a novel regulator in the control of interfascicular cambium activity and secondary xylem formation in Arabidopsis. In particular, in inflorescence stems of *ahl15* loss-of-function mutant plants, we observed a delay in cambium ring initiation and formation and a significant reduction in the amount of secondary xylem formed. By contrast, inflorescence stems of *AHL15* overexpression plants developed an increased amount of secondary xylem. Our data suggest that the *AHL15* gene is a positive regulator of cambial cell proliferation and thereby an important determinant of secondary xylem formation in Arabidopsis inflorescence stems.

AHL15 belongs to a large family of *AHL* genes in Arabidopsis that have a high degree of functional redundancy among family members.[21] Our recent observations indicate that *AHL15* acts redundantly with other *AHL* genes in controlling embryogenesis[27] and AM maturation.[28] For secondary growth, however, we observed a significant reduction in the *ahl15* loss-of-function mutant background, and introduction of the *ahl15* mutation in the woody *soc1 ful* double mutant background reduced secondary growth to almost wild-type levels, indicating that *AHL15* is a key regulator of this process downstream of SOC1 and FUL (Figure 6). A similar central role for AHL15 was observed in short day-repressed AM maturation in Arabidopsis.[28]

Cell proliferation in the cambial zone is known to be controlled by both genetic and hormonal factors.[1,8,14] Based on the current model, the TDIF-PXY-WOX and cytokinin/auxin pathways act in parallel to regulate cell division in the vascular cambium (Figure 6).[1] In the first pathway, the TDIF peptide, belonging to the CLE family of peptides, is produced in the phloem and subsequently transferred to the cambium where it binds to the PXY receptor-like kinase. Upon peptide binding, PXY activates the expression of the cambium-specific transcription factors WOX4 and WOX14, which promote cell proliferation in the cambium (Figure 6). Our results lead to a model where AHL15 promotes the timing of cambial cell initiation, proliferation, and maintenance in parallel to and dependent on the TDIF-PXY-WOX pathway by increasing the expression of cytokinin biosynthesis genes (Figure 6). Interestingly, it has been shown that the cambial cell division and secondary xylem production are significantly increased upon elevated cytokinin levels in stems of poplar trees.[14] Moreover, AHL3-AHL4 heterodimers have been reported to control the boundary between the procambium and xylem axis in Arabidopsis roots.[25] Single and double loss-of-function mutants of *AHL3* and *AHL4* display ectopic protoxylem vessels and ectopic metaxylem vessels in the procambial region adjacent to the xylem axis.[25] Since the cytokinin response is altered in the *ahl4* loss-of-function mutant and similar vascular defects have been observed for cytokinin-defective mutants,[25] this confirms the strong relationship between *AHL* genes and cytokinin in cambium initiation and cell division and in the resulting xylem formation. Cytokinin likely influences the cell cycle of the cambium stem cells by modulating the expression of D-type cyclins,[17,18] but how exactly cytokinin promotes cambial cell divisions and its interaction with auxin in this process are still not fully understood. The SOC1/FUL-AHL15-cytokinin pathway in our model might join with the auxin and PXY-WOX pathways at the TMO6-WOX14-LBD4 feedforward loop that was recently proposed.[43] This would nicely explain the interdependency of the different pathways in regulating cambium activity.

Interestingly, we also observed a role for *AHL15* in promoting lateral branching, as loss of function resulted in a reduced number and overexpression in an increased number of lateral

(D) Confocal images showing the activity of $WOX4_{pro}$*:GFP* in the main inflorescence stem of wild-type (upper panel) and *ahl15* (lower panel) plants 10 or 18 days after bolting. xy, xylem; ph, phloem; c, cambium; if, intravascular fiber. Images represent an overlay of the green (GFP) and red (chlorophyll) fluorescence channels.

Scale bars, 0.06 mm (B) and 0.03 mm (D). For (B) and (D), similar results were obtained from two independent experiments.

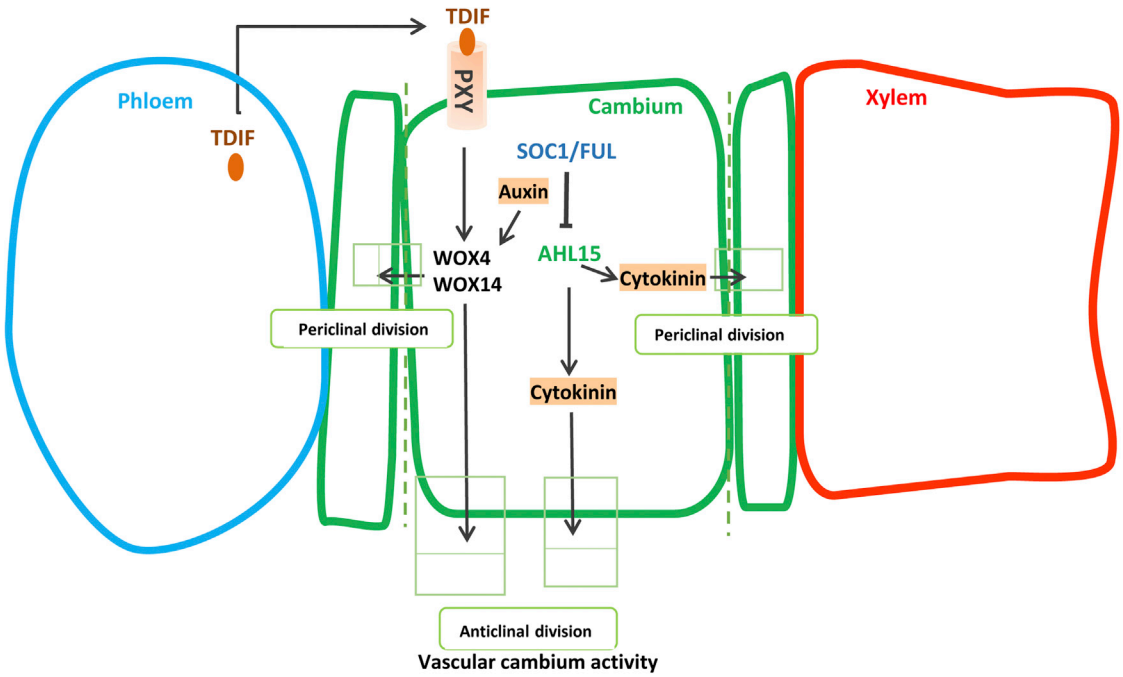

Figure 6. Model for the key role of *AHL15* in promoting cambium activity

Schematic drawing of the cambium area showing the phloem (blue), cambium (green), and xylem (red) cell types. Peptide TDIF is synthesized in the phloem and travels through the apoplastic space to the cambium cells, where it is recognized by the PXY receptor. PXY subsequently promotes periclinal and anticlinal cell division activity of cambium cells by activating the expression of *WOX4* and *WOX14*. Auxin also promotes cambium cell proliferation by enhancing *WOX* gene expression through MP/ARF5. In a parallel pathway, the MADS box transcription factors SOC1 and FUL limit cambium activity by repressing *AHL15* expression. AHL15, in turn, promotes cell division activity of the cambium by enhancing the expression of cytokinin biosynthesis genes. Blunt-ending lines indicate repression; arrows indicate promotion.

branches. AM-specific *AHL15* overexpression led to enhanced expression of the cytokinin biosynthesis genes *LOG5*, *IPT3*, and *IPT7*, which makes it tempting to speculate that cytokinin is also downstream of *AHL15* in this process. It has been reported that cytokinin promotes shoot branching by repressing *BRC1* expression, which activates axillary buds.[44,45] It is therefore very possible that *AHL15* and cytokinin act in the same pathway in regulating cambium and AM activity.

In conclusion, we show that *AHL* genes positively regulate both cambium activity and AM outgrowth[28] in Arabidopsis, downstream of the SOC1 and FUL transcription factors. Our previous studies have shown that the *AHL* gene family can be found in both annual and perennial plant species and that perenniality is not linked to an increase in *AHL* gene copy number, but rather to enhanced *AHL* expression.[28] Similarly, *AHL* expression levels are likely to differentiate between herbaceous or woody stem growth. Our findings represent an important step forward in our understanding of the increased vascular cambium activity and shoot branching. In particular, they show that it is possible to increase secondary growth without affecting the flowering time and fruit and seed development of plants, which will eventually be helpful to improve crop biomass production or drought resilience.[4,14,46]

STAR★METHODS

Detailed methods are provided in the online version of this paper and include the following:

SUPPLEMENTAL INFORMATION

Supplemental information can be found online at https://doi.org/10.1016/j.cub.2022.02.060.

ACKNOWLEDGMENTS

We thank Niharika Savant and Floor van der Klauw for generating the constructs *PXY-AHL15* and *PXY-IPT*, respectively, and Gerda Lammers and Merijn de Bakker for their help with microscopy. We are grateful to Ward de Winter, Jan Vink, Nick Surtel, and Mariel Lavrijsen for their technical support. O.K. was supported in part by grant G14_006.02 to R.O. from Generade, and by the

Building Blocks of Life grant 737.016.013 to R.O. from the Dutch Research Council. D.S. was supported by a postdoctoral fellowship of the Japan Society for the Promotion of Science (JSPS Overseas Research Fellowships 201960008) and a JST PRESTO grant (JPMJPR2046). O.N. was funded by the Ministry of Education, Youth and Sports of the Czech Republic (project no. CZ.02.1.01/0.0/0.0/16_019/0000827) and by an Internal Grant of Palacký University in Olomouc (IGA_PrF_2022_016). Work in T.G.'s lab was supported by the European Research Council (ERC) through an ERC Consolidator grant (647148, PLANTSTEMS) and the Deutsche Forschungsgemeinschaft (DFG) through project grant GR2104/7-1.

AUTHOR CONTRIBUTIONS

A.R., O.K., and R.O. designed experiments and analyzed results. A.R. performed the majority of the experiments. A.D.L. analyzed the *PXY$_{pro}$:AHL15* Arabidopsis lines. T.d.W. analyzed and did qPCR analysis on the *MYB2$_{pro}$:AHL15* lines. P.A. and O.N. performed cytokinin measurements and analyzed the data. D.S. and T.G. generated the tissue-specific gene expression atlas from different Arabidopsis stem tissues. O.K. and R.O. supervised the project. A.R., O.K., and R.O. wrote the manuscript. All authors read, commented on, and approved the content of the manuscript.

DECLARATION OF INTERESTS

The authors declare no competing interests.

Received: April 12, 2021
Revised: December 10, 2021
Accepted: February 22, 2022
Published: March 15, 2022

REFERENCES

1. Fischer, U., Kucukoglu, M., Helariutta, Y., and Bhalerao, R.P. (2019). The dynamics of cambial stem cell activity. Annu. Rev. Plant Biol. *70*, 293–319.
2. Jouannet, V., Brackmann, K., and Greb, T. (2015). (Pro)cambium formation and proliferation: two sides of the same coin? Curr. Opin. Plant Biol. *23*, 54–60.
3. Dória, L.C., Meijs, C., Podadera, D.S., Del Arco, M., Smets, E., Delzon, S., and Lens, F. (2019). Embolism resistance in stems of herbaceous Brassicaceae and Asteraceae is linked to differences in woodiness and precipitation. Ann. Bot. *124*, 1–14.
4. Thonglim, A., Delzon, S., Larter, M., Karami, O., Rahimi, A., Offringa, R., Keurentjes, J.J.B., Balazadeh, S., Smets, E., and Lens, F. (2020). Intervessel pit membrane thickness best explains variation in embolism resistance amongst stems of *Arabidopsis thaliana* accessions. Ann. Bot. *128*, 1–12.
5. Tonn, N., and Greb, T. (2017). Radial plant growth. Curr. Biol. *27*, R878–R882.
6. Ragni, L., and Greb, T. (2018). Secondary growth as a determinant of plant shape and form. Semin. Cell Dev. Biol. *79*, 58–67.
7. Nieminen, K., Blomster, T., Helariutta, Y., and Mähönen, A.P. (2015). Vascular cambium development. Arabidopsis Book *13*, e0177.
8. Oles, V., Panchenko, A., and Smertenko, A. (2017). Modeling hormonal control of cambium proliferation. PLoS One *12*, e0171927.
9. Etchells, J.P., and Turner, S.R. (2010). The PXY-CLE41 receptor ligand pair defines a multifunctional pathway that controls the rate and orientation of vascular cell division. Development *137*, 767–774.
10. Hirakawa, Y., Kondo, Y., and Fukuda, H. (2010). TDIF peptide signaling regulates vascular stem cell proliferation via the WOX4 homeobox gene in Arabidopsis. Plant Cell *22*, 2618–2629.
11. Wang, N., Bagdassarian, K.S., Doherty, R.E., Kroon, J.T., Connor, K.A., Wang, X.Y., Wang, W., Jermyn, I.H., Turner, S.R., and Etchells, J.P. (2019). Organ-specific genetic interactions between paralogues of the PXY and ER receptor kinases enforce radial patterning in Arabidopsis vascular tissue. Development *146*, 10.1242.
12. Zhou, Y., Liu, X., Engstrom, E.M., Nimchuk, Z.L., Pruneda-Paz, J.L., Tarr, P.T., Yan, A., Kay, S.A., and Meyerowitz, E.M. (2015). Control of plant stem cell function by conserved interacting transcriptional regulators. Nature *517*, 377–380.
13. Bhalerao, R.P., Fischer, U., and Turner, S. (2016). Environmental and hormonal control of cambial stem cell dynamics. J. Exp. Bot. *68*, 79–87.
14. Immanen, J., Nieminen, K., Smolander, O.P., Kojima, M., Alonso Serra, J., Koskinen, P., Zhang, J., Elo, A., Mähönen, A.P., Street, N., et al. (2016). Cytokinin and auxin display distinct but interconnected distribution and signaling profiles to stimulate cambial activity. Curr. Biol. *26*, 1990–1997.
15. Brackmann, K., Qi, J., Gebert, M., Jouannet, V., Schlamp, T., Grünwald, K., Wallner, E.S., Novikova, D.D., Levitsky, V.G., Agustí, J., et al. (2018). Spatial specificity of auxin responses coordinates wood formation. Nat. Commun. *9*, 875.
16. Miyawaki, K., Tarkowski, P., Matsumoto-Kitano, M., Kato, T., Sato, S., Tarkowska, D., Tabata, S., Sandberg, G., and Kakimoto, T. (2006). Roles of Arabidopsis ATP/ADP isopentenyltransferases and tRNA isopentenyltransferases in cytokinin biosynthesis. Proc. Natl. Acad. Sci. USA *103*, 16598–16603.
17. Dewitte, W., Scofield, S., Alcasabas, A.A., Maughan, S.C., Menges, M., Braun, N., Collins, C., Nieuwland, J., Prinsen, E., Sundaresan, V., and Murray, J.A.H. (2007). Arabidopsis CYCD3 D-type cyclins link cell proliferation and endocycles and are rate-limiting for cytokinin responses. Proc. Natl. Acad. Sci. USA *104*, 14537–14542.
18. Randall, R.S., Miyashima, S., Blomster, T., Zhang, J., Elo, A., Karlberg, A., Immanen, J., Nieminen, K., Lee, J.Y., Kakimoto, T., et al. (2015). AINTEGUMENTA and the D-type cyclin CYCD3;1 regulate root secondary growth and respond to cytokinins. Biol. Open *4*, 1229–1236.
19. Melzer, S., Lens, F., Gennen, J., Vanneste, S., Rohde, A., and Beeckman, T. (2008). Flowering-time genes modulate meristem determinacy and growth form in *Arabidopsis thaliana*. Nat. Genet. *40*, 1489–1492.
20. Fujimoto, S., Matsunaga, S., Yonemura, M., Uchiyama, S., Azuma, T., and Fukui, K. (2004). Identification of a novel plant MAR DNA binding protein localized on chromosomal surfaces. Plant Mol. Biol. *56*, 225–239.
21. Zhao, J., Favero, D.S., Peng, H., and Neff, M.M. (2013). *Arabidopsis thaliana* AHL family modulates hypocotyl growth redundantly by interacting with each other via the PPC/DUF296 domain. Proc. Natl. Acad. Sci. USA *110*, E4688–E4697.
22. Street, I.H., Shah, P.K., Smith, A.M., Avery, N., and Neff, M.M. (2008). The AT-hook-containing proteins SOB3/AHL29 and ESC/AHL27 are negative modulators of hypocotyl growth in Arabidopsis. Plant J. *54*, 1–14.
23. Xiao, C., Chen, F., Yu, X., Lin, C., and Fu, Y.-F. (2009). Over-expression of an AT-hook gene, AHL22, delays flowering and inhibits the elongation of the hypocotyl in *Arabidopsis thaliana*. Plant Mol. Biol. *71*, 39–50.
24. Ng, K.-H., Yu, H., and Ito, T. (2009). AGAMOUS controls *GIANT KILLER*, a multifunctional chromatin modifier in reproductive organ patterning and differentiation. PLoS Biol. *7*, e1000251.
25. Zhou, J., Wang, X., Lee, J.-Y., and Lee, J.-Y. (2013). Cell-to-cell movement of two interacting AT-hook factors in Arabidopsis root vascular tissue patterning. Plant Cell *25*, 187–201.
26. Matsushita, A., Furumoto, T., Ishida, S., and Takahashi, Y. (2007). AGF1, an AT-hook protein, is necessary for the negative feedback of *AtGA3ox1* encoding GA 3-oxidase. Plant Physiol. *143*, 1152–1162.
27. Karami, O., Rahimi, A., Mak, P., Horstman, A., Boutilier, K., Compier, M., Van der Zaal, B., and Offringa, R. (2021). An Arabidopsis AT-hook motif nuclear protein mediates somatic-to-embryonic cell fate conversion coinciding with genome duplication. Nat. Commun. *12*, 2508.
28. Karami, O., Rahimi, A., Khan, M., Bemer, M., Hazarika, R.R., Mak, P., Compier, M., van Noort, V., and Offringa, R. (2020). A suppressor of axillary meristem maturation promotes longevity in flowering plants. Nat. Plants *6*, 368–376.
29. Altamura, M.M., Possenti, M., Matteucci, A., Baima, S., Ruberti, I., and Morelli, G. (2001). Development of the vascular system in the inflorescence stem of Arabidopsis. New Phytol. *151*, 381–389.

30. Shi, D., Jouannet, V., Agustí, J., Kaul, V., Levitsky, V., Sanchez, P., Mironova, V.V., and Greb, T. (2021). Tissue-specific transcriptome profiling of the Arabidopsis inflorescence stem reveals local cellular signatures. Plant Cell *33*, 200–223.

31. Shi, D., Lebovka, I., López-Salmerón, V., Sanchez, P., and Greb, T. (2019). Bifacial cambium stem cells generate xylem and phloem during radial plant growth. Development *146*, 1–8.

32. Fisher, K., and Turner, S. (2007). PXY, a receptor-like kinase essential for maintaining polarity during plant vascular-tissue development. Curr. Biol. *17*, 1061–1066.

33. Benková, E., Michniewicz, M., Sauer, M., Teichmann, T., Seifertová, D., Jürgens, G., and Friml, J. (2003). Local, efflux-dependent auxin gradients as a common module for plant organ formation. Cell *115*, 591–602.

34. Zürcher, E., Tavor-Deslex, D., Lituiev, D., Enkerli, K., Tarr, P.T., and Müller, B. (2013). A robust and sensitive synthetic sensor to monitor the transcriptional output of the cytokinin signaling network in planta. Plant Physiol. *161*, 1066–1075.

35. Matsumoto-Kitano, M., Kusumoto, T., Tarkowski, P., Kinoshita-Tsujimura, K., Václavíková, K., Miyawaki, K., and Kakimoto, T. (2008). Cytokinins are central regulators of cambial activity. Proc. Natl. Acad. Sci. USA *105*, 20027–20031.

36. Tokunaga, H., Kojima, M., Kuroha, T., Ishida, T., Sugimoto, K., Kiba, T., and Sakakibara, H. (2012). Arabidopsis lonely guy (LOG) multiple mutants reveal a central role of the LOG-dependent pathway in cytokinin activation. Plant J. *69*, 355–365.

37. Kuroha, T., Tokunaga, H., Kojima, M., Ueda, N., Ishida, T., Nagawa, S., Fukuda, H., Sugimoto, K., and Sakakibara, H. (2009). Functional analyses of LONELY GUY cytokinin-activating enzymes reveal the importance of the direct activation pathway in Arabidopsis. Plant Cell *21*, 3152–3169.

38. Aguilar-Martínez, J.A., Poza-Carrión, C., and Cubas, P. (2007). Arabidopsis BRANCHED1 acts as an integrator of branching signals within axillary buds. Plant Cell *19*, 458–472.

39. González-Grandío, E., Pajoro, A., Franco-Zorrilla, J.M., Tarancón, C., Immink, R.G.H., and Cubas, P. (2017). Abscisic acid signaling is controlled by a BRANCHED1/HD-ZIP i cascade in Arabidopsis axillary buds. Proc. Natl. Acad. Sci. USA *114*, E245–E254.

40. Guo, Y., and Gan, S. (2011). AtMYB2 regulates whole plant senescence by inhibiting cytokinin-mediated branching at late stages of development in Arabidopsis. Plant Physiol. *156*, 1612–1619.

41. Etchells, J.P., Provost, C.M., Mishra, L., and Turner, S.R. (2013). WOX4 and WOX14 act downstream of the PXY receptor kinase to regulate plant vascular proliferation independently of any role in vascular organisation. Development *140*, 2224–2234.

42. Suer, S., Agusti, J., Sanchez, P., Schwarz, M., and Greb, T. (2011). WOX4 imparts auxin responsiveness to cambium cells in Arabidopsis. Plant Cell *23*, 3247–3259.

43. Smit, M.E., McGregor, S.R., Sun, H., Gough, C., Bågman, A.M., Soyars, C.L., Kroon, J.T., Gaudinier, A., Williams, C.J., Yang, X., et al. (2020). A PXY-mediated transcriptional network integrates signaling mechanisms to control vascular development in Arabidopsis. Plant Cell *32*, 319–335.

44. Dun, E.A., de Saint Germain, A., Rameau, C., and Beveridge, C.A. (2012). Antagonistic action of strigolactone and cytokinin in bud outgrowth control. Plant Physiol. *158*, 487–498.

45. Ferguson, B.J., and Beveridge, C.A. (2009). Roles for auxin, cytokinin, and strigolactone in regulating shoot branching. Plant Physiol. *149*, 1929–1944.

46. Dória, L.C., Podadera, D.S., del Arco, M., Chauvin, T., Smets, E., Delzon, S., and Lens, F. (2018). Insular woody daisies (Argyranthemum, Asteraceae) are more resistant to drought-induced hydraulic failure than their herbaceous relatives. Funct. Ecol. *32*, 1467–1478.

47. Chen, J., Li, Y., Zhang, K., and Wang, H. (2018). Whole-genome sequence of phage-resistant strain *Escherichia coli* DH5α. Genome Announc. *6*, e00097–e00018.

48. Lazo, G.R., Stein, P.A., and Ludwig, R.A. (1991). A DNA transformation-competent Arabidopsis genomic library in Agrobacterium. Biotechnology (N Y) *9*, 963–967.

49. Murashige, T., and Skoog, F. (1962). A revised medium for rapid growth and bio assays with tobacco tissue cultures. Physiol. Plant. *15*, 473–497.

50. Müller, B., and Sheen, J. (2008). Cytokinin and auxin interplay in root stem-cell specification during early embryogenesis. Nature *4*, 1094–1097.

51. Van Der Graaff, E.E., Auer, C.A., and Hooykaas, P.J.J. (2001). Altered development of *Arabidopsis thaliana* carrying the *Agrobacterium tumefaciens ipt* gene is partially due to ethylene effects. Plant Growth Regul. *34*, 305–315.

52. den Dulk-Ras, A., and Hooykaas, P.J. (1995). Electroporation of *Agrobacterium tumefaciens*. Methods Mol. Biol. *55*, 63–72.

53. Clough, S.J., and Bent, A.F. (1998). Floral dip: a simplified method for Agrobacterium-mediated transformation of *Arabidopsis thaliana*. Plant J. *16*, 735–743.

54. Livak, K.J., and Schmittgen, T.D. (2001). Analysis of relative gene expression data using real-time quantitative PCR and the 2(-Delta Delta C(T)) method. Methods *25*, 402–408.

55. Zhang, G., Zhao, M., Song, C., Luo, A., Bai, J., and Guo, S. (2012). Characterization of reference genes for quantitative real-time PCR analysis in various tissues of Anoectochilus roxburghii. Mol. Biol. Rep. *39*, 5905–5912.

56. Mitra, P.P., and Loqué, D. (2014). Histochemical staining of *Arabidopsis thaliana* secondary cell wall elements. J. Vis. Exp. e51381.

57. Anandalakshmi, R., Pruss, G.J., Ge, X., Marathe, R., Mallory, A.C., Smith, T.H., and Vance, V.B. (1998). A viral suppressor of gene silencing in plants. Proc. Natl. Acad. Sci. USA *95*, 13079–13084.

58. Svačinová, J., Novák, O., Plačková, L., Lenobel, R., Holík, J., Strnad, M., and Doležal, K. (2012). A new approach for cytokinin isolation from Arabidopsis tissues using miniaturized purification: pipette tip solid-phase extraction. Plant Methods *8*, 17.

59. Antoniadi, I., Plačková, L., Simonovik, B., Doležal, K., Turnbull, C., Ljung, K., and Novák, O. (2015). Cell-type-specific cytokinin distribution within the Arabidopsis primary root apex. Plant Cell *27*, 1955–1967.

STAR★METHODS

KEY RESOURCES TABLE

REAGENT or RESOURCE	SOURCE	IDENTIFIER
Bacterial and virus strains		
E. coli DH5a	Chen et al.[47]	GenBank: CP026085
Agrobacterium tumefaciens AGL1	Lazo et al.[48]	N/A
Chemicals, peptides, and recombinant proteins		
Dexamethasone	Sigma-Aldrich	D4902
Phloroglucinol	Sigma-Aldrich	P3502-25G
Toluidine blue	Sigma-Aldrich	T3260-5G
Ethanol 96% GPR Rectapur	VWR	20824.365
Acetone Analar Normapur	VWR	20066.330
½ MS medium	Murashige and Skoog[49]	N/A
	Duchefa	M0222.0100
X-gluc	Thermo Fischer Scientific	R0852
Daishin Plant Agar	Duchefa	Cat#P1004.5000
Critical commercial assays		
RNeasy Mini kit	Qiagen	ID: 74904
RevertAid Reverse Transcription kit	Thermo Fischer Scientific	K1691
SYBR green master-mix	Thermo Fischer Scientific	4309155
Experimental models: Organisms/strains		
Arabidopsis thaliana Col-0	NASC (http://arabidopsis.info/)	N1092
Arabidopis ahl15	Karami et al.[28]	N/A
Arabidopis soc1-6 ful-7	Karami et al.[28]	N/A
Arabidopis pxy wox4 wox14	Etchells et al.[41]	N/A
Arabidopis AHL15$_{pro}$:AHL15	Karami et al.[28]	N/A
Arabidopis 35S$_{pro}$:AHL15-GR	Karami et al.[28]	N/A
Arabidopis AHL15$_{pro}$:GUS	Karami et al.[28]	N/A
Arabidopis ahl15/+, AHL15$_{pro}$:AHL15-ΔG	Karami et al.[28]	N/A
Arabidopis PXY$_{pro}$:AHL15	This paper	N/A
Arabidopis MYB2$_{pro}$:AHL15	This paper	N/A
Arabidopis DR5$_{pro}$:GFP	Benková et al.[33]	N/A
Arabidopis TCS$_{pro}$:GFP	Müller and Sheen [50]	N/A
Arabidopis WOX4$_{pro}$:YFP	Suer et al.[42]	N/A
Oligonucleotides		
Primers used for cloning, genotyping and qRT-PCR	Table S1, this paper	N/A
Recombinant DNA		
pDONR207	Novopro	V011826
PXY$_{pro}$:IPT	This paper	N/A
PXY$_{pro}$:AHL15	This paper	N/A
MYB2$_{pro}$:AHL15	This paper	N/A
pGW-AHL15	Karami et al.[28]	N/A
Software and algorithms		
GraphPad Prism 8	GraphPad Software, USA	https://www.graphpad.com
CLC Main Workbench	Qiagen Digitalinsights	https://digitalinsights.qiagen.com
Bio-Rad CFX manager 3.1	Bio-Rad	https://www.bio-rad.com
ImageJ	Open source	https://imagej.nih.gov/ij
Target Lynx V4.2	Waters	https://www.waters.com/

RESOURCE AVAILABILITY

Lead contact

Further information and requests for resources and reagents should be directed to and will be fulfilled by the lead contact, Remko Offringa (r.offringa@biology.leidenuniv.nl).

Materials availability

All unique/stable reagents generated in this study are available from the lead contact without restriction.

Data and code availability

- Microscopy, qPCR, cytokinin quantification and plant phenotyping data reported in this paper will be shared by the lead contact upon request.
- This paper does not report original code.
- Any additional information required to reanalyze the data reported in this paper is available from the lead contact upon request.

EXPERIMENTAL MODEL AND SUBJECT DETAILS

Arabidopsis growth conditions

Seeds were surface sterilized with 40% (v/v) bleach solution followed by four times washing with sterile water and germinated, after three days incubation at 4°C, on ½ MS[49] medium containing 1% (w/v) sucrose and grown at 21°C, 65% relative humidity and a 16 hours (long day: LD) photoperiod (100 to 120 μMol/m^2.s lightintensity), and plants were photographed with a Nikon D5300 camera. For dexamethasone (DEX, Sigma-Aldrich) treatment, the bottom-most internode of the main inflorescence stem of *35S$_{pro}$:AHL15-GR* plants was sprayed with 20 μM DEX.

Plant material

All Arabidopsis mutant- and transgenic lines used in this study (see key resources table) are in the Columbia (Col-0) background. New mutant combinations listed in the key resources table were obtained by crossing and several rounds of genotyping (using primer combinations listed in Table S1), phenotyping (reporter detection or selection for resistance marker) and self pollination until plant lines homozygous for all mutant and transgene loci were obtained.

METHOD DETAILS

Gene names used in this paper

Named genes in this paper correspond to the following proteins and genes (listed as TAIR/UniProt: gene name, UniProt ID, TAIR: locus ID): *AtAHL15*, Q9M2S3, AT3G55560; *AtFUL*, T2CBN1, AT5G60910; *AtIPT3*, Q9C6L1-1, AT3G63110; *AtIPT7*, Q9C6L1-1, AT3G23630; *AtLOG4*, Q8RUN2-1, AT3G53450; *AtLOG5*, Q8LBB7, AT4G35190; *AtMYB2*, Q9SPN3, AT2G47190; *AtPXY*, Q9FII5, AT5G61480; *AtSOC1*, Q9XID9-1, AT2G45660; *AtWOX4*, Q6X7J9, AT1G46480; *AtWOX14*, Q9LM83-1, AT1G20700.

Plasmid construction and Arabidopsis transformation

Molecular cloning was predesigned *in silico* using CLC Main Workbench. To generate the *PXY$_{pro}$:AHL15* or *MYB2$_{pro}$:AHL15* constructs, an upstream region of approximately 3 kb from the ATG initiation codon of the *PXY (AT5G61480)* or the *MYB2(AT2G47190)* genes were amplified from ecotype Columbia (Col-0) genomic DNA using the forward (F) and reverse (R) PCR primers indicated in Table S1. The resulting fragment was first recombined into pDONR207 by a BP reaction, its integrity was checked by sequence analysis and the fragment was subsequently cloned upstream of the *AHL15* cDNA fragment in previously made destination vector *pGW-AHL15.*[28] by a LR reaction according to Gateway cloning procedures (Clonetech). To generate the *PXY$_{pro}$:IPT* construct, the *AHL15* gene in the *PXY$_{pro}$:AHL15* construct was replaced by a *Kpn*I and *Xba*I flanked fragment containing the *IPT* gene from *Agrobacterium tumefaciens.*[51] All binary vectors were checked for integrity by restriction enzyme and PCR analysis and introduced into *Agrobacterium tumefaciens* strain AGL1 by electroporation.[52] Subsequently, Arabidopsis Col-0, *ahl15*, and *wox4wox14pxy* plants were transformed using the floral dip method.[53] Hygromycin resistant T1 plants were grown and at least four independent transgenic lines with a single locus T-DNA insertion were selected and self-pollinated to generate homozygous transgenic lines. Transgene function and expression was verified by qPCR and phenotypic analysis of the resulting plants.

RNA preparation and quantitative real-time PCR (qRT-PCR)

RNA was isolated from the rosette base, and the bottom-most internode of inflorescence stems (about 0.5 cm above rosette base) using the RNeasy kit (Qiagen), and quantified using a Nanodrop 1000 spectrophotometer (Thermo Scientific). First-strand cDNA was synthesized from 1 μg RNA using the RevertAid RT Reverse Transcription kit (Thermo Fischer Scientific) with 1μl of the oligo (dT)

primer. Quantitative PCR was performed on three biological replicates along with three technical replicates in a 10μl reaction containing 0.5μMol of both forward and reverse primer and 5μl of the SYBR-green dye premixed master-mix (Thermo Fischer Scientific. The primers used for each gene are described in Table S1. PCR reactions were performed in a C1000 Touch thermal cycler (BIO-RAD) by incubation at 50°C for 2 min, 95°C for 10 min and 40 cycles of 95°C for 15s and 60°C for 1 min. PCR amplicon identity was verified by heating from 60°C to 95°C with ramp speed of 1.9°C min-1, resulting in melting curves. CT values were obtained using Bio-Rad CFX manager 3.1. The relative expression level of genes was calculated according to the $2^{-\Delta\Delta Ct}$ method,[54] and expression was normalized using the *β-TUBULIN-6* gene as a Zhang et al.[55]

Histology and microscopy

To analyze stem secondary growth and lignification, the bottom-most internode of the main inflorescence stem was cut and sectioned freshly using a razor blade (Wilkinson Sword). Very thin-fresh free-hand cross-sections were kept on ice until the staining in 3% (w/v) phloroglucinol-HCL (0.3 g phloroglucinol, 10 ml absolute ethanol, 5 ml 37 % (v/v) HCL), using a protocol from Mitra and Loqué.[56] Sections were further analyzed under a light microscope (Nikon eclipse Ci-E/Ci-L). The secondary xylem width was measured with ImageJ for three randomly selected interfascicular parts of the individual stem and the average value was calculated per plant per stem. For embedded sections, the bottom-most internodes of 1- or 2-month-old main inflorescence stems (of at least 1 cm long, including the stem base) were harvested and fixed overnight in 4 % formaldehyde in a 50 mM phosphate solution. The stems were dehydrated in a graded ethanol series (70 %, 80 %, 90 %, 96 %, 100 % (v/v)) and embedded in epoxy resin molds. Sections (3-4μm) were made using a rotary microtome (Leica RM2265) and subsequently stained in 0.01 % (w/v) toluidine blue (in water), before being analyzed under a light microscope (Nikon eclipse Ci-E/Ci-L).

Histochemical β-glucuronidase (GUS) staining was performed as described previously.[57] Bottom-most internodes were cut one centimeter above the rosette base and placed in tubes containing cold acetone 90% on ice. Following vacuum infiltration while keeping them on ice, samples were washed two times in GUS staining solution without X-gluc and subsequent vacuum infiltration, after which they were transferred to GUS staining solution with 1 mg/ml X-gluc (Thermo Fischer). After vacuum infiltration, the staining reaction was allowed to proceed for approximately 2 hours at 37°C in the dark. After rehydration in a graded ethanol series (75, 50, and 25 % (v/v)), the stained tissues were cut freshly by razor blade (very thin-fresh free-hand cross-sections) and observed and photographed using a light microscope (Nikon eclipse Ci-E/Ci-L). At least seven independent plants were analyzed for each time point. GFP expression was visualized in fresh free-hand cross sections of inflorescence stems that were placed on a microscopy slide covered with coverslip using the ZEISS-003-18533 confocal laser scanning microscope equipped with a 534 nm laser, a 488 nm long pass excitation filter and 500-525 nm band pass emission filters.

Cytokinin quantification

Quantification of cytokinin metabolites were performed in five independent biological replicates according to the method described by Svačinová et al.,[58] including modifications described by Antoniadi et al.[59] Samples (10 mg fresh weight) were homogenized and extracted in 1 ml of modified Bieleski buffer (60% MeOH, 10% HCOOH and 30% H_2O (v/v)). A mixture of stable isotope-labeled internal standards (0.2 pmol of CK bases, ribosides, *N*-glucosides, and 0.5 pmol of CK *O*-glucosides, nucleotides per sample added) was added to validate the liquid chromatography-electrospray tandem mass spectrometry (LC-MS/MS) method. The extracts were applied onto an Oasis MCX column (30 mg/1 ml, Waters) conditioned with 1 ml each of 100% methanol and H_2O, equilibrated sequentially with 1ml of 50% (v/v) nitric acid, 1 ml of H_2O, and 1 ml of 1M HCOOH, and washed with 1 ml of 1M HCOOH and 1 ml 100% methanol. Analytes were then eluted by two-step elution using 1 ml of 0.35M NH_4OH aqueous solution and 2 ml of 0.35M NH_4OH in 60% (v/v) MeOH solution. The eluates were evaporated to dryness *in vacuo* and then dissolved in 40 μL of 10% methanol prior to LC-MS/MS analysis. The chromatographic separation (10-μL injection of each sample) was performed using an Acquity I-Class system (Waters, Milford, MA, USA) equipped with an Acquity UPLC BEH Shield RP18 column (150 × 2.1 mm, 1.7 μm; Waters). Effluent was analyzed using triple quadrupole mass spectrometer (Xevo TQ-S, Waters) equipped with electrospray ionization source. Data were processed with Target Lynx V4.2 software and final concentration levels of cytokinin metabolites were determined.

QUANTIFICATION AND STATISTICAL ANALYSIS

RT-PCR data, cytokinin measurements and countings of lateral branches per plant (as defined in Figure S6A) were imported into excel and statistically analyzed by a two-sided Student's t test. The radial width of the interfascicular xylem was measured in ImageJ using images of toluidine blue- or phloroglucinol-stained cross sections of the bottom-most internode of inflorescence stems, data were statistically analyzed in GraphPad Prism 8 by a one-way ANOVA with Tukey's honest significant difference post hoc test. Data from the previous tissue-specific transcriptome profiling of the Arabidopsis inflorescence stem[30] were compared using the likelihood ratio test. All data were plotted into graphs using GraphPad Prism 8.